Impact of stator segmentation on forces and vibrations in PM generators for offshore wind power

Klop, Casper L. ; Dong, Jianning; Olsen, Pål Keim

DOI
10.1049/icp.2023.1972

Publication date
2023

Document Version
Final published version

Published in
Proceedings of the 12th International Conference on Power Electronics, Machines and Drives (PEMD 2023)

IMPACT OF STATOR SEGMENTATION ON FORCES AND VIBRATIONS IN PM GENERATORS FOR OFFSHORE WIND POWER

Casper L. Klop [1], Jianning Dong[2], Pål Keim Olsen[1]*

[1]*Electrical Power Engineering, Norwegian University of Science and Technology, Trondheim, Norway*
[2]*DC Systems, Energy Conversion & Storage, Delft University of Technology, Delft, The Netherlands*
**casper.klop@ntnu.no*

Keywords: HVDC, MODULARITY, WIND POWER, FORCES, VIBRATIONS

Abstract

The ModHVDC concept is a modular permanent magnet generator which uses insulated stator segments with dedicated power electronic converters to produce HVDC. This could significantly reduce the number of required power conversion steps for HVDC-connected offshore wind parks. However, the concept poses structural challenges to the machine design, which are investigated in this paper. It is observed that segmentation of the stator has two major effects on the harmonic forces that occur inside in the machine: the addition of low spatial order harmonics, referred to as the segment harmonics, and an increase of the cogging torque. Furthermore, the structural integrity of the stator was found to be reduced. Based on these findings, design recommendations are put forward to mitigate the drawbacks of stator segmentation.

1 Introduction

Offshore wind power is projected to play a major role in the rapid energy transition and decarbonization efforts toward 2050. As wind farms are built increasingly far from shore, the Inter-national Energy Agency (IEA) has identified improving High-Voltage Direct Current (HVDC) transmission infrastructure as a key innovation requirement to reduce cost and improve efficiency [1]. The modular HVDC drive (ModHVDC) concept has been proposed to reduce the number of power conversion stages between the wind farms and the HVDC transmission grid in [2, 3]. This concept uses insulated stator segments that have a dedicated Power Electronic Converter of which the DC outputs are connected in series to produce HVDC. Additional benefits include a reduced nacelle mass by mitigating the need for a transformer as well as an improved fault tolerance by simplifying stator maintenance and enabling the possibility to bypass a faulty stator module.

The forces on the stator have been identified as a challenge for the ModHVDC concept, as the insulation leads to gaps between the stator segments which act as flux barriers. Research in [4,5] has indicated that these flux barriers influence the forces that occur in small modular machines. In addition, [6] has shown that Direct-Drive Wind Turbine Generators (DD-WTGs) with open slots require special attention with regards to their slot harmonics. Thus far, the only study into the structural aspects of a modular DD-WTG neglected the effect of slotting and did not study the vibrations in the machine in detail [7]. To address this gap, this paper provides a detailed analysis of the impact of segmentation on the harmonic forces and the structural response of a modular electric machine.

This work is based on the preliminary work of a thesis [8] and presents an extended analysis to provide the key findings of the project. Figure 1 shows the method used in this study. Section 2 introduces the machine model that is used in section 3 to calculate the electromagnetic forces based on the magnetic flux distribution. These forces are applied to a structural model in section 4. Combining the electromagnetic and structural analysis shows the existence of *segment harmonics* that cause vibrations of the same order of magnitude as the slot harmonics, which is explained in section 5.

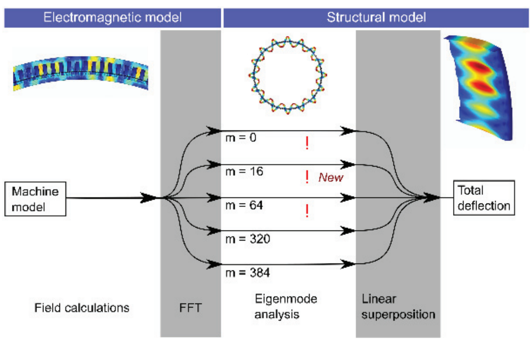

Fig. 1 The method used in this study.

2 Machine Design

The machine parameters used in this study can be found in Table 1. The machine is simulated in COMSOL Multiphysics to confirm it meets the design goals without exceeding saturation and loading limits. Single-layer, fractional- slot concentrated windings (FSCW) are used to enable physical modularity. For the given design, the machine has a periodicity

https://doi.org/10.1049/icp.2023.1972

Table 1 Machine parameters

Design goals	
	Value *(per segment)*
Electrical Power P	10 MW *(625 kW)*
RMS Phase voltage V_{ph}	42.8 kV *(2.67 kV)*
Rotation speed S	10 RPM
Machine layout	
Number of slots N_s	384 *(24)*
Number of pole pairs p	160 *(10)*
Number of segments N_{seg}	16
Geometric parameters	
Outer rotor radius R_{ro}	4.85 m
Outer stator radius R_{so}	5.0 m
Active length L	1.7 m
Air gap g	10 mm
Magnet length l_m	30 mm
Tooth width w_{th}	39 mm
Average slot width w_s	41 mm
Slot depth d_s	63 mm
Gap between segments w_{gap}	10 mm
Electromagnetic parameters	
PM remanence B_r	1.2 T
Electrical frequency f_c	26.7 Hz
Turns per slot n_s	61
RMS coil current i	92.4 A
Power factor cos φ	0.85
Frame parameters	
Frame thickness h_f	5 mm
Frame length L_f	2.0 m
Press fit interference δ	5 mm
Material properties	
Core in-plane Young's modulus E_p	180 GPa
Core out-of-plane Young's modulus E_z	100 GPa
Core density ρ_c	7700 kg/m^3
Frame Young's modulus E_f	200 GPa
Frame density ρ_f	7850 kg/m^3

F1 = 32, which results in subharmonics in the magnetic field of the stator. Two different designs are considered for the steel frame that holds the segments in position, which are presented in Section IV.

3 Electromagnetic Analysis and Force Calculations

The magnetic flux distribution B is analysed both analytically in MATLAB and numerically in COMSOL. In both cases, the resulting forces *f* are calculated using a simplified form of the Maxwell stress tensor. Using a complex notation of the radial and tangential components of both B and *f*, this relation is given by (1) [9].

$$f = f_r + jf_t = \frac{1}{2\mu_0}B^2 \quad \text{with} \quad B = B_r + jB_t \qquad (1)$$

For most machines, B_t is negligible since the flux density lines are nearly perpendicular to the stator teeth [10].

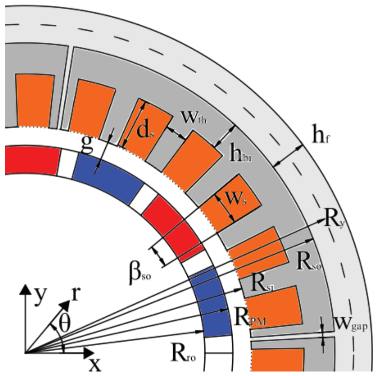

Fig. 2 The layout of the machine with its design parameters.

However, for large machines with open slots, the contribution of the tangential magnetic fields can be substantial [6] and is therefore included in this analysis.

3.1 Analytical Method

The analytical analysis, available online at [11], is based on the method outlined in [10]. It is improved with the slotless magnetic field equations given in [12–14] for radially magnetized surface-mounted permanent magnets on the rotor and [15–17] for concentrated windings in the stator. This method breaks down the total magnetic field and force distribution into *spatial radial orders* m, which refers to the number of peaks and troughs along the machine circumference. The influence of the open slots is calculated by using a complex relative air gap permeance λ_s, which is calculated using the method proposed in [18].

The real and imaginary components of $\lambda_s = \lambda_{a,s} + j\lambda_{b,s}$ are expressed as Fourier series, which for regular stators have a fundamental order equal to the number of slots N_s. This paper proposes to analyse the impact of segmentation by modelling the insulated gap between two stator segments in the same way as the slots, namely by imagining the segment gap as a small slot between very wide teeth. This results in a complex relative permeance λ_{gap} with a fundamental order equal to the number of segments N_{seg}. λ_{gap} is then superimposed on λ_s to obtain $\lambda = \lambda_a + j\lambda_b$, whose components are described by (2). The result, given in Fig. 3, shows the segment gap close to $\theta = 3\pi/32$.

$$\lambda_a(\theta) = \lambda_0 + \sum_{i=1}^{N_\lambda} \lambda_{a.si}\cos(iN_s\theta) + \sum_{i=1}^{N_\lambda} \lambda_{a.gapi}\cos(iN_{seg}\theta)$$

$$\lambda_b(\theta) = \sum_{i=1}^{N_\lambda} \lambda_{b.si}\sin(iN_s\theta) + \sum_{i=1}^{N_\lambda} \lambda_{b.gapi}\sin(iN_{seg}\theta) \qquad (2)$$

The obtained relative permeance is then used to calculate the slotted flux density distribution in the air gap using (3) [14, 18]. If saturation is neglected, this equals the linear superposition of the rotor and stator field.

$$B = B_{slotless}\lambda^* = (B^{PM}_{slotless} + B^{arm}_{slotless})\lambda^* \qquad (3)$$

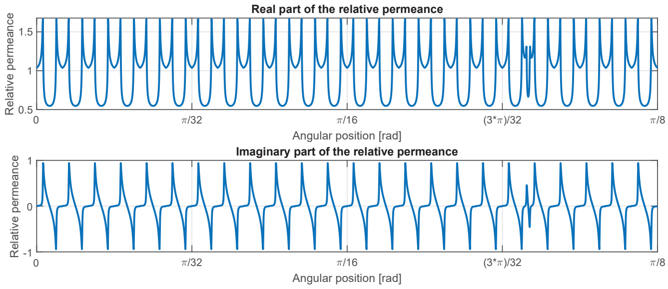

Fig. 3 The real and imaginary part of the relative permeance for 1 segment, taking both slots and flux gaps into account.

3.2 Numerical Method
A 2D numerical model is set up in COMSOL Multiphysics using the parameters given in Table 1. By using symmetric boundary conditions, a single segment can be simulated. The electrical steel is modelled using a B-H curve to include saturation in the model, but steel losses are neglected. The magnetic fields are simulated using a time-stepping analysis, where the rotor is modelled as a rotating mesh and the phase currents are set in the q-axis. The resulting forces are again calculated using Maxwell's stress tensor.

4 Structural Analysis

A modal analysis is used to evaluate the structural response of the machine. In this analysis, a linear superposition of structural eigenmodes is assumed. These are excited by forces with the same radial spatial order and amplified if the excitation frequency is close to the eigenfrequency [10]. Two design options are considered to analyse the impact of stator segmentation. In the first design (Fig. 4, l), the stator segments are pressed into the frame and held in position by friction, resembling what has been used in small modular machines [5]. In the second design (Fig. 4, r), the stator segments are constrained by beams, which allows for a gap between the frame and stator that can be used for cooling [19]. The number and location of the beams was varied to study their effect.

4.1 Approach
The eigenmodes of the system and the deflections caused by the electromagnetic forces are studied by implementing structural 3D models in COMSOL. The stator laminations are modelled using equivalent orthotropic material properties based on [20, 21]. The press-fit design is modelled using an additional static analysis in which the interference δ between the stator and frame is translated into a prestress. Then, this prestressed condition is used as linearization point for the eigenmode analysis. After the eigenmode analysis, the forces found in Section III are applied to the teeth as a Boundary Load in the frequency domain.

The numerical model is compared to an analytical model based on Donnel-Mushtari's theory for thin cylinders [10], which showed similar results within a margin of ±30%. The analytical results are expected to be inaccurate due to the assumption of isotropic materials and the uncertainty of the level of coupling between the stator and frame. Both models

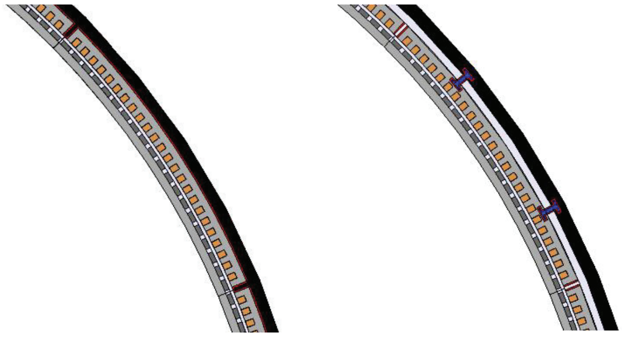

Fig. 4 Left: design 1, using an interference fit. Right: design 2, using support beams (both figures not to scale).

show that the quasi-static deflection amplitude A_m of a mode m, neglecting resonance, reduces rapidly for increasing m, in the order of $A_m \propto m^{-4}$. This demonstrates that it is crucial to consider forces with low spatial orders, even when their amplitudes are relatively small.

5 Results

This section presents the results of the electromagnetic and structural analysis described above. Subsection 5.1 gives an overall overview of the force density harmonics in the machine, 5.2 and 5.3 show the two main electromagnetic effects of segmentation, and Subsection 5.4 discusses the structural response.

5.1 Resulting Force Density Harmonics
Equation (1) shows that the force distribution is the result of interactions between flux density waves. Specifically, when B is given as a Fourier series with spatial orders k, f becomes the sum of force harmonics m which are generated by the sum of all pairs of flux density harmonics for which holds that $|k_1 \pm k_2| = m$. Machines with concentrated windings generally have a rich harmonic spectrum of forces due to the low $\gcd(Ns, p)$ and the subharmonics in the armature reaction [6, 22, 23]. Table 2 summarizes the most important force density harmonics. For the tangential forces, similar harmonics are present.

Table 2 Summary of resulting radial force density harmonics

Type	Spatial order	Frequency	Comments
Breathing mode	0	Mainly $6\omega_e$	Low for sinusoidal currents
Due to slotless PM fields	$2kp$	$2k\omega_e$	Dominant in most machines
Due to slotless armature fields	$2kF1$	$2\omega_e$	Only present in on-load case
Due to interactions of PM harmonic μ and armature harmonic ν	$\mu p \pm \nu F1$	$(\mu \pm 1)\omega_e$	Only present in on-load case
Slot harmonics	$2kF1$	Mainly $2\omega_e$	Adds low-order harmonics
Segment harmonics	kN_{seg}	Mainly $2\omega_e$	Creates very low order harmonics
For $k = 1, 2, 3, \ldots$			

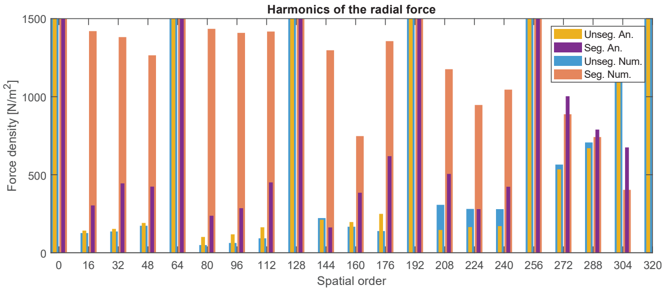

Fig. 5 The analytical and numerical lower spatial orders of the segmented and the unsegmented machine.

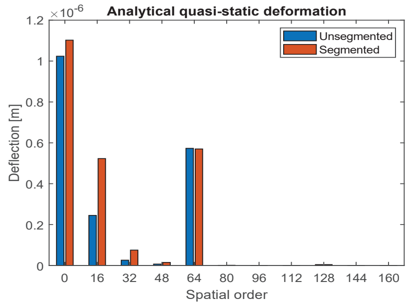

Fig. 7 Analytical results for the quasi-static deformation.

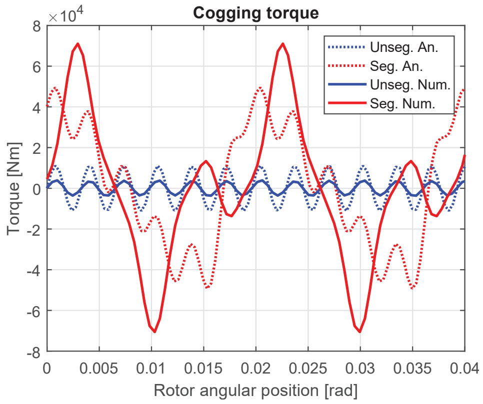

Fig. 6 The analytical and numerical cogging torque of the segmented and the unsegmented machine.

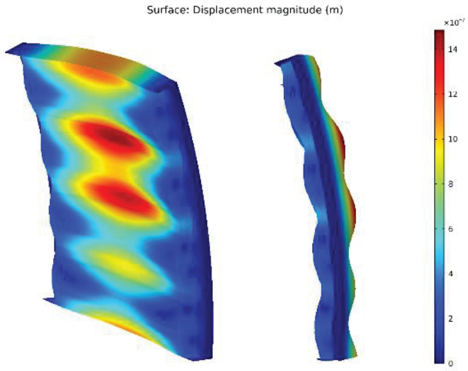

Fig 8 The numerical deflection, neglecting the constant pressure.

5.2 Segment Harmonics

First, the analytical method predicts that the additional harmonics in the air gap permeance due to the segment gaps result in force harmonics with spatial orders at multiples of $\gcd(p, N_{seg})$. These harmonics are similar to how slots cause a slot harmonic at multiples of $\gcd(p, N_s)$ [6, 14]. Due to symmetry conditions, $\gcd(p, N_{seg}) = N_{seg}$, which means these *segment harmonics* have a very low spatial order as shown in Fig. 5. This means that the segment harmonics can lead to significant structural vibrations, even if the force amplitude is low.

The numerical simulation shows these segment harmonics as well, but with a significantly higher amplitude than predicted by the analytical model. This higher amplitude is explained by a change in magnetic flux distribution inside the stator due to the flux barriers, which slightly change the winding factors of low spatial harmonics. This is similar to what was observed in [4, 5].

5.3 The Effect of Segmentation on the Cogging Torque

Secondly, segmentation increases the cogging torque, the torque in the no-load case caused by the interaction of the PMs and the slots. The cogging torque of a machine is strongly influenced by $N_L = \mathrm{lcm}(N_s, 2p)$ [9, 24, 25], with a higher N_L leading to a higher frequency and a lower amplitude. The segment gaps will result in an additional cogging torque with a frequency of $\mathrm{lcm}(N_{seg}, 2p)$ which equals $2p$ due to symmetry conditions.

Thus, according to the analytical method, segmentation decreases the fundamental cogging frequency and increases its amplitude, comparable to what was observed in [26]. The numerical analysis confirms a significantly increased cogging torque due to the segment gaps, as shown in Fig. 6. Since the cogging torque remains below 1% of the nominal torque, the effect of this increase is expected to be limited.

5.4 Structural Response

The structural response of both designs is dominated by three vibrations modes: the breathing mode $m = 0$, the segment harmonic $m = 16$ and the slot harmonic $m = 64$, analytically shown in Fig. 7. Despite its far smaller force amplitude, the segment harmonic results in vibration amplitudes in the same order of magnitude as the slot harmonic. This is explained by the $A_m \propto m^{-4}$ relation mentioned before.

Benchmarking the eigenmode analysis to a non-segmented machine revealed that segmentation has a limited effect on the structural integrity of the first design, since the segments and frame are still fully coupled. The structural response is shown in Fig. 8, in which the segment and slot harmonic can be recognized. In the second design, the structural response is highly dependent on the specific way in which the segments are constrained. As lower vibration modes generally have lower stiffness, the $m = 16$ mode already has a relatively low eigenfrequency. If the segments are constrained in such a way that the structure has a low stiffness in this mode, the associated eigenfrequency approaches the excitation frequency of $2\omega_e = 53$ Hz and vibration displacements become an order of magnitude larger than for the press fit design.

The eigenfrequency of the structural breathing mode is close to the excitation frequency of $6\omega_e = 160$ Hz, and is therefore amplified. The last important vibration mode, $m = 64$, is primarily important due to the large force amplitude of the slot harmonic, which results from the use of concentrated windings.

6 Conclusion and Recommendations

This paper studied the impact of stator segmentation on the harmonic forces and their resulting mechanical vibrations in large PM generators for HVDC-connected offshore wind power. Overall, a very rich harmonic force spectrum was observed, due to the use of concentrated windings in a large, open-slot machine.

The effect of segmentation on the harmonic forces was found to be twofold. First, segmentation adds force harmonics with a very low spatial order, identified as segment harmonics in this paper. Although the amplitude of these forces is small, the relatively low stiffness of the stator for modes with lower radial orders result in vibrations of the same order of magnitude as those generated by the slot harmonics. Second, the amplitude of the cogging torque was found to be increased, and its periodicity reduced. Both effects were partially predicted by the proposed analytical model, and found to be more pronounced in the numerical analysis. To improve the accuracy of the analytical model, it is recommended to calculate the winding factors for the segmented machine numerically as suggested by [27] and to include the effects of flux (de)focusing as suggested by [5].

The structural impact of segmentation was found to be strongly dependent on its exact design. For designs in which the segments are rigidly connected to the frame, the structural integrity of the machine is maintained. For designs that allow more movement of the segments, it is recommended to ensure sufficient stiffness of the eigenmodes that can be excited by the segment harmonics.

6 References

[1] IEA. Offshore Wind Outlook 2019: World Energy Outlook Special Report. International Energy Agency, 2019.

[2] Olsen, P. K.: "Energy Conversion System". WIPO WO 2012/093942 Al, 2012.

[3] da Rocha, L. F., Faraasen, H.A., Vansompel, H., Olsen, P.K. "Investigation of Power Electronics Converters and Architecture for Modular HVDC Wind Generators". In: IEEE Int. Conf. on Power Systems Tech. 2022, pp. 1–6.

[4] Dajaku, G., Xie, W., and Gerling, D. "Reduction of low space harmonics for the fractional slot concentrated windings using a novel stator design". In: IEEE Trans. Magn., 2013, 50 (5), pp 1-12.

[5] Li, G. J., Zhu, Z. Q., Chu, W. Q., Foster, M. P., & Stone, D. A. "Influence of flux gaps on electromagnetic performance of novel modular pm machines". In: IEEE Trans. Energy Convers. 29 (3 2014), pp. 716–726.

[6] Valavi, M., Nysveen, A., Nilssen, R., & Rølvåg, T. "Slot harmonic effect on magnetic forces and vibration in low-speed permanent-magnet machine with concentrated windings". In: IEEE Trans. Ind. Appl. 50 (5 Sept. 2014), pp. 3304–3313.

[7] Shipurkar, U., Wani, F., Dong, J., Alpogiannis, G., Polinder, H., Bauer, P., & Ferreira, J. A. "Comparison of Modular Wind Turbine Generators Considering Structural Aspects". In: Proc. Annu. Conf. IEEE Ind. Electron. Soc. (IECON) (2017), pp. 3707–3712.

[8] Klop, C. "Forces and vibrations in a Modular HVDC Generator". Master thesis, Delft University of Technology, Sept. 2022. URL: http://resolver.tudelft.nl/uuid:f8fdcfb6-c05a-4a1f-873b-26f7c8409d68.

[9] Besnerais, J. L. "Vibroacoustic analysis of radial and tangential airgap magnetic forces in permanent magnet synchronous machines". In: IEEE Trans. Magn. 51 (6 June 2015), pp 1-9.

[10] Gieras, J. F., Wang, C., and Lai, J. C. Noise of Polyphase Electric Motors. CRC Press, Oct. 2018.

[11] Klop, C. L. Harmonic Analysis of ModHVDC Generator. Version 1.0.0. Aug. 2022. URL: https://github.com/CasperKlop/Thesis.

[12] Zhu, Z. Q., Howe, D., Bolte, E., & Ackermann, B. "Instantaneous Magnetic Field Distribution in Brushless Permanent Magnet DC Motors, Part I: Open-Circuit Field". In: IEEE Trans. Magn. 29 (1 1993), pp. 124–135.

[13] Zhu, Z. Q., Howe, D., and Chan, C. C. "Improved analytical model for predicting the magnetic field distribution in brushless permanent-magnet machines". In: IEEE Trans. Magn. 38 (1 II Jan. 2002), pp. 229–238.

[14] Zhu, Z. Q., Xia, Z. P., Wu, L. J., & Jewell, G. W. "Analytical modeling and finite-element computation of radial vibration force in fractional-slot permanent-magnet brushless machines". In: IEEE Trans. Ind. Appl. 46 (5 Sept. 2010), pp. 1908–1918.

[15] Krøvel, O. Design of Large Permanent Magnetized Synchronous Electric Machines. 2011. URL: http://hdl.handle.net/11250/256994.

[16] Zhu, Z. Q. and Howe, D. "Instantaneous Magnetic Field Distribution in Brushless Permanent Magnet DC Motors, Part II: Armature-Reaction Field". In: IEEE Trans. Magn. 29 (1 1993), pp. 136–142.

[17] Yokoi, Y., Higuchi, T., and Miyamoto, Y. "General Formulation of Winding Factor for Fractional-Slot Concentrated Winding Design". In: IET Electr. Power Appl. 10 (4 2016), pp. 231–239.

[18] Žarko, D., Ban, D., and Lipo, T. A. "Analytical calculation of magnetic field distribution in the slotted air gap of a surface permanent-magnet motor using complex relative air-gap permeance". In: IEEE Trans. Magn. 42 (7 July 2006), pp. 1828–1837.

[19] Lyngved, K. H. and Olsen, P. K. Investigating Thermal Management Solutions in a Modular High Voltage Machine for Offshore Wind Application. Master thesis, NTNU, 2021. URL: https://hdl.handle.net/11250/2824803.

[20] Giet, M., Kasper, K., De Doncker, R. W., & Hameyer, K. "Material parameters for the structural dynamic simulation of

electrical machines". In: Proc. Int. Conf. Electr. Mach. (ICEM) (2012), pp. 2994–3000.
[21] Saito, A., Nishikawa, Y., Yamasaki, S., Fujita, K., Kawamoto, A., Kuroishi, M., & Nakai, H. "Equivalent orthotropic elastic moduli identification method for laminated electrical steel sheets". In: Mech. Syst. Sig. Process. 72-73 (May 2016), pp. 607–628.
[22] Bianchi, N., Bolognani, S., Pre, M. D., & Grezzani, G. A. G. G. "Design considerations for fractional-slot winding configurations of synchronous machines". In: IEEE Trans. Ind. Appl. 42 (4 July 2006), pp. 997–1006.
[23] Valavi, M., Nysveen, A., Nilssen, R., Lorenz, R. D., & Rølvåg, T. "Influence of pole and slot combinations on magnetic forces and vibration in low-speed PM wind generators". In: IEEE Trans. Magn. 50 (5 2014).
[24] Hwang, S. M., Eom, J. B., Jung, Y. H., Lee, D. W., & Kang, B. S. "Various design techniques to reduce cogging torque by controlling energy variation in permanent magnet motors". In: IEEE Trans. Magn. 37 (4 I July 2001), pp. 2806–2809.
[25] Zhu, Z. Q. and Howe, D. "Influence of design parameters on cogging torque in permanent magnet machines". In: IEEE Trans. Energy Convers. 15 (4 Dec. 2000), pp. 407–412.
[26] Zhu, Z. Q., Azar, Z., and Ombach, G. "Influence of additional air gaps between stator segments on cogging torque of permanent-magnet machines having modular stators". In: IEEE Trans. Magn. 48 (6 2012), pp. 2049–2055.
[27] Heins, G., Ionel, D. M., and Thiele, M. "Winding Factors and Magnetic Fields in Permanent-Magnet Brushless Machines With Concentrated Windings and Modular Stator Cores". In: IEEE Trans. Ind. Appl. 51.4 (2015), pp. 2924–2932.